

Atomistic modelling of radiation damage in zircon

Kostya O Trachenko^{1,2}, Martin T Dove^{1,3} and Ekhard K H Salje¹

¹ Mineral Physics Group, Department of Earth Sciences, University of Cambridge, Downing Street, Cambridge CB2 3EQ, UK

² Cavendish Laboratory, University of Cambridge, Madingley Road, Cambridge CB3 0HE, UK

E-mail: martin@esc.cam.ac.uk (M T Dove)

Received 30 October 2000, in final form 18 January 2001

Abstract

We report the results of simulation of radiation damage in zircon structure using the molecular dynamics technique. The phases of the damage production process, including the ballistic and thermal spike phases, are detected, quantified and visualized. We find that the higher ambient temperature results in substantial decrease of the damage throughout the damage production process. We simulate the overlap of the displacement cascades and find that the damaged structure is less able to resist the damage, in that more damage is produced in the structure that is already damaged and the relaxation time increases. The calculated density of the damaged structure shows the increase in the core of the damaged region. We relate this densification to the appearance of chains of connected SiO_n polyhedra in the damaged structure. The number of connected polyhedra increases with the increase of the damage, consistently with recent nuclear magnetic resonance results. ‘Polymers’ of connected SiO_n are found to be essentially stable on annealing for the timescales available in computer simulations and their alignment may possess the ‘memory’ of the alignment of SiO_4 tetrahedra in crystalline zircon.

1. Introduction

Zircon, ZrSiO_4 , has been widely studied recently because of its response to radiation damage. The interest is generated by several important applications in which zircon is exposed to radiation, including using natural zircon in geochronology and as a host material to immobilize radioactive nuclear materials and waste. During an internal alpha-decay event the energetic recoil atom produces a displacement cascade of about 1000 atoms and the alpha particle produces several hundred isolated atomic displacements. At high radiation doses zircon becomes heavily damaged, or metamict, as judged from the diffraction experiments [1–3]. Recent experimental work has concentrated on the nature of the radiation damage in zircon on a macroscopic level [4–8].

³ Author to whom any correspondence should be addressed.

To model the macroscopic effects of radiation damage, we proposed a general stress model of irradiated material discussed previously [9]. This model, applicable to any material under irradiation, allowed us to study the mechanism of macroscopic volume swelling, percolation of damaged and crystalline regions, and adequately reproduced scattering profiles observed experimentally [7, 8].

In recent years, atomistic simulations of radiation damage effects have been intensively employed, for they addressed the processes of radiation damage that happen over scales of length and time that are small by the standards of experiment, i.e. nm and ps respectively. On that scale, the so-called primary damage process takes place during which damage is produced in the structure. Atomistic modelling of radiation damage in zircon has been rather limited. The first attempts to simulate radiation damage in zircon on an atomistic level using molecular dynamics were carried out by Crocombette and Ghaleb [10, 11]. They studied the local temperature in the core of the displacement cascade and in the periphery. At early stages of the damage production process the temperature in the core was found to be larger than the melting temperature of zircon. The number of atoms displaced by the radiation events was calculated at the final stage of the damage production process. In the core of the displacement cascade the crystalline structure was found to be completely lost. Finally, it was pointed out that in the damaged region Si atoms may connect to each other by sharing common oxygen atoms. The evolution of radiation damage in zircon was addressed by Park *et al* [12], using molecular dynamics simulation.

In this paper we present further detailed analysis of the radiation damage in zircon using molecular dynamics simulation. We study the response of the structure of zircon to radiation impact at different ambient temperatures. The phases of damage production are observed and quantified, including the ballistic phase, during which the energy of the recoil atom is distributed among many atoms and the disordered region is created, and the thermal spike phase, during which the kinetic and potential components of the crystal energy attain equilibrium with each other and relaxation of the ‘hot’ disordered region takes place. It is demonstrated that the higher temperatures significantly reduce the number of atoms displaced by the radiation damage event. We simulate the overlap of the displacement cascades by implanting several radiation events at adjacent sites of the simulation box and find that a damaged structure appears to be less resistant to further radiation damage, in that more damage is created by an event with the same energy and the relaxation time increases. The damage production process is displayed in the form of MPEG animations.

We observe the structural changes beyond the creation of disorder, particularly the appearance of ‘polymers’ of connected SiO_n polyhedra, $n = 4, 5, 6$, that are vertex or edge linked. The number of polyhedra connected in ‘polymers’ increases as more damage is introduced in the structure, consistently with recent NMR measurements [13, 14]. We find that while the density of the damaged region becomes close to that of the crystalline one at the boundaries of the region, the density in the region’s core is increased over the density of the crystalline region. We relate this densification to the appearance of connected chains of SiO_n polyhedra.

2. Methods

In modelling atomic interactions in zircon, we used potentials for Si and O atoms from the simulation of quartz [15]. They included the pair Buckingham potential acting between Si–O atoms:

$$U(r_{ij}) = A \exp\left(-\frac{r_{ij}}{\rho}\right) - \frac{C}{r_{ij}^6} \quad (1)$$

and the three-body potential with parameters selected to keep the O–Si–O angle in the SiO₄ tetrahedron at approximately 109°. Si–O interactions were complemented with the Zr–O potential from a simulation of ZrW₂O₈ in the form of a pair Buckingham potential [16]. Zr, Si and O atoms were assigned formal Coulomb charges, 4.0, 4.0 and –2.0, respectively. The parameters of the Buckingham potentials of the Si–O, Zr–O and O–O atomic interactions are listed in table 1.

Table 1. Parameters of the Buckingham potential employed for the Si–O, Zr–O and O–O interactions in zircon.

	A (eV)	ρ (Å)	C (eV Å ⁶)
Si–O	1354.9546	0.3104097	5.33
Zr–O	8000000	0.14	0
O–O	22764	0.149	27.879

In order to validate the model of zircon, the energy optimization was performed using the package GULP [17]. The experimental values of unit-cell parameters, bond lengths and bond angles were compared with the calculated optimized values. The comparison is presented in table 2. As can be seen from table 2, the agreement between the experimental and calculated values is good.

Table 2. The comparison of experimental values of unit-cell parameters and bond lengths with the calculated optimized values.

	Experimental value	Calculated value	Difference (%)
Unit-cell parameters			
a, b	6.604 Å	6.520 Å	–1.27
c	5.979 Å	6.095 Å	1.94
Bond lengths			
Si–O	1.623 Å	1.614 Å	0.55
Zr–O1	2.128 Å	2.137 Å	0.42
Zr–O2	2.267 Å	2.231 Å	1.59
Bond angles			
O–Si–O (1)	97°	95°	–2
O–Si–O (2)	116°	117°	0.9

We used the DLPOLY molecular dynamics simulation package [19]. A structure containing 8640 atoms was equilibrated at 300 K and 600 K, and one atom (usually called the primary knock-on atom and chosen to be Zr in our case) was given a velocity corresponding to an implantation energy of about 1 keV. Computational limits prevented us from using higher values for the energy. We employed different integration algorithms, including coupling the system to Nose–Hoover and Berendsen thermostats. The choice of algorithm proved to have little effect on the results. Periodic boundary conditions were applied. It should be noted that the energy damping at the boundaries is often employed to prevent the kinetic disturbances from re-entering the simulation box. However, as was demonstrated in [20, 21], the use of periodic boundaries is acceptable if the size of the simulation cell is large enough, which was the case in our simulations.

3. Damage production and relaxation

A sequence of snapshots of the sample containing the displacement cascade at different times is shown in figure 1, showing how damage develops in the structure. The energy of the primary knock-on atom is distributed, by multiple collisions, among surrounding atoms which leave their lattice sites. This results in the creation of a highly damaged core surrounded by relatively undistorted regions which move outwards, with the number of displaced atoms reaching its maximum at about 0.15 ps (figure 1). A substantial fraction of displaced atoms return to their original positions during a period of several ps. The atoms that are unable to occupy their original lattice sites form a displacement cascade, with a high degree of topological disorder in the core, which is stable during times of simulation of 100 ps. The animations showing the creation and development of displacement cascades are available in MPEG format in the electronic version of this journal and can be downloaded from <http://www.esc.cam.ac.uk/movies>.

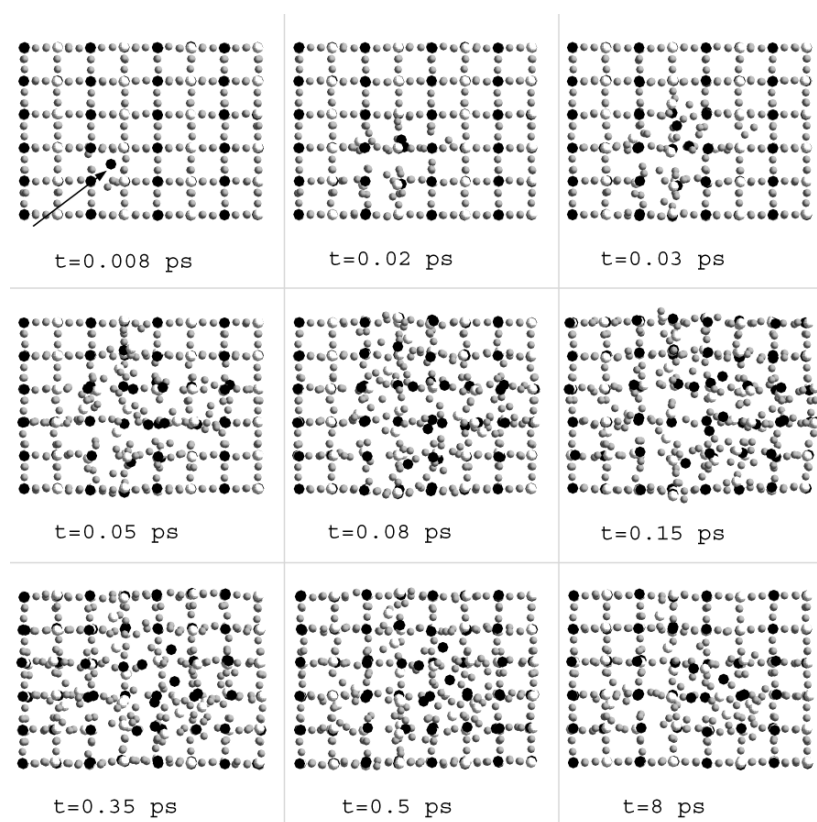



Figure 1. Snapshots of zircon structure showing the development of a displacement cascade in time (viewed along [001]). The arrow shows the direction of velocity of the primary knock-on atom. Larger black and white balls represent Zr and Si atoms respectively, and smaller grey atoms represent O atoms. Animations of the damage production process in zircon at different temperatures are available in the MPEG format in the electronic version of the journal (see below). They can also be viewed from <http://www.esc.cam.ac.uk/movies>.

 An MPEG movie of this figure is available from the article's abstract page in the online journal; see www.iop.org.

Various criteria are used to identify atoms as displaced from their original positions by a radiation impact [22]. We consider an atom as being displaced if it leaves the sphere centred at its initial lattice position with the radius of half a nearest-neighbour distance. The number of displaced atoms, N_d , was averaged over seven different events simulated by giving the primary knock-on atom different velocity components. We plot N_d as a function of time in figure 2 for Zr, Si and O atoms simulated at 300 K and 600 K. One can observe N_d reaching its maximum value at about 0.15 ps, corresponding to the maximum in disorder in figure 1. After this phase, known as the thermal spike, N_d becomes a constant value at about 0.5 ps and 1 ps for simulations at 300 K and 600 K, respectively.

Comparing figures 2(a) and 2(b) makes it apparent that the temperature has a significant effect on N_d both during the thermal spike phase and for longer times. The total number of displaced atoms is about 1.8 larger in the sample at 300 K than at 600 K. This effect is believed to be due to the increase in the lifetime of the thermal spike as the temperature increases, which allows more defect motion to take place before cooling and hence leads to more interstitial–vacancy recombination [21, 23]. The increase in the lifetime of the thermal spike phase with temperature can be seen in figure 2. This feature is consistent with the results of simulation of damage production in metals [21, 23]. The interesting point from figure 2 is that N_d is also lower at the higher temperature at the times corresponding to the maximum of N_d and the thermal spike. This is different from the results of simulation of radiation damage in metals [21, 23], which showed that as the initial temperature increases, N_d decreases at the final stages of damage production, but increases during the thermal spike phase.

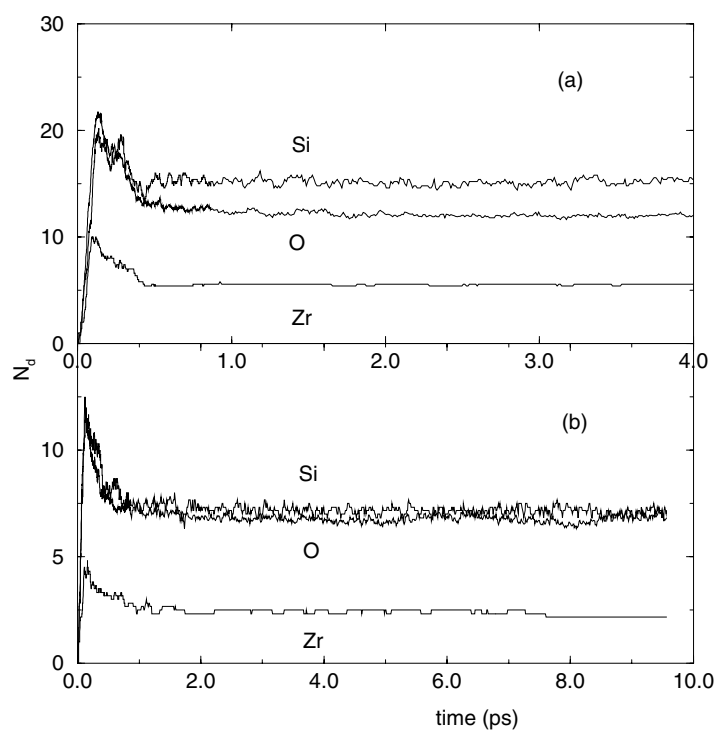


Figure 2. Number of displaced atoms as a function of time during the simulation at (a) 300 K and (b) 600 K. To facilitate comparison with other atoms, the number of displaced oxygen atoms was divided by 4.

4. Repeated radiation events

In order to study the structural changes in the damaged zircon, density variation and other features, a damaged region of an appropriate size defined by the locations of displaced atoms is required. A single radiation event, even with a high energy, may not be suitable for this purpose. The reason for this is that in the region with the linear size defined by the maximal spatial separation of two displaced atoms in the cascade, there are still a substantial fraction of atoms located on the crystalline lattice sites. In order to address the properties of the damaged region, the majority of atoms in that region should be displaced. This called for the simulation of several consecutive radiation events implanted at the adjacent regions of the simulation box. Besides, it was appealing to study the effect of the overlap of displacement cascades.

To simulate consecutive radiation events, the initial velocities of the primary knock-on atoms were directed approximately at the centre of the selected region in the simulation box. After simulating the ballistic phase and relaxation of one radiation event, the structure was equilibrated at 300 K before implanting the next primary knock-on atom. A number of consecutive radiation events produced a damaged region with dimensions of about $30 \times 20 \times 20 \text{ \AA}^3$ that contained several hundred displaced atoms (as defined above).

We plot the radial distribution function (rdf) calculated for the displaced atoms in the damaged region, together with the one calculated for the atoms on undistorted lattice sites, in figure 3. It can be seen that rdf of displaced atoms preserved only two well-defined maxima, corresponding to the nearest Si–O and O–O distances in crystalline zircon. This suggests that the displaced atoms may be grouped into tetrahedral-like formations. Later in this paper we will see that the damaged structure contains chains of connected SiO_n , $n = 4, 5, 6$, polyhedra.

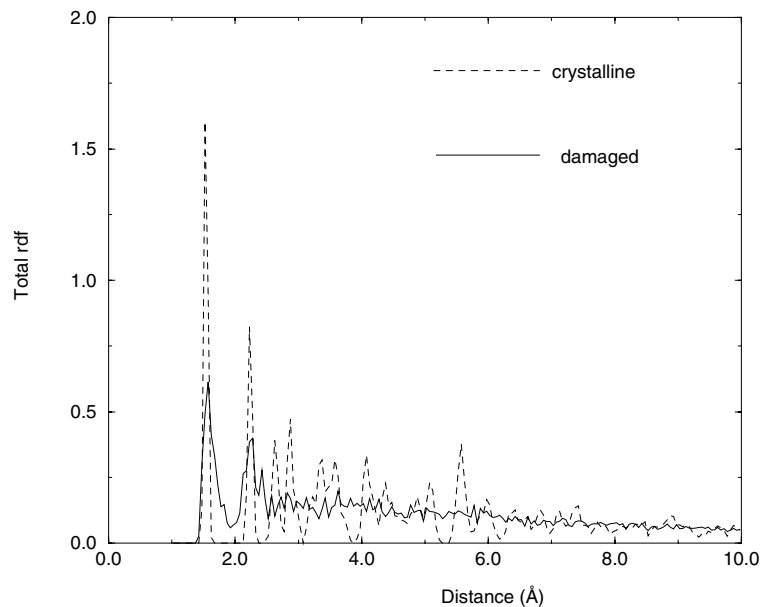


Figure 3. Total radial distribution functions calculated for displaced atoms in the damaged and undistorted regions.

It is interesting to note the difference in the dependence of N_d on time t between the first event presented in figure 2(a) and the subsequent events. The dependence of N_d on t calculated for the fourth event is presented in figure 4(a). Note that N_d was calculated by comparing the

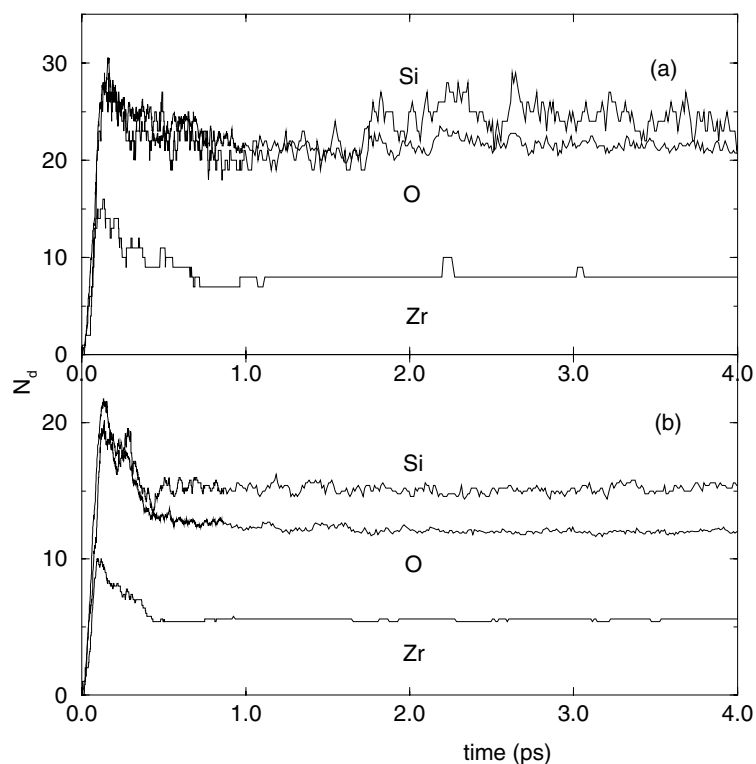


Figure 4. Number of displaced atoms as a function of time during the simulation of (a) the fourth consecutive radiation event and (b) the single radiation event (as in figure 2(a)). To facilitate comparison with other atoms, the number of displaced oxygen atoms was divided by 4.

number of displaced atoms with the configuration immediately preceding the fourth event, and not with the initial undistorted configuration. For comparison, $N_d = N_d(t)$ for the single event is shown in figure 4(b) (as in figure 2(a)). In the repeated event the primary knock-on atom and the front of the displacement cascade move towards a region of which the major part is already damaged by the previous radiation events. As can be seen from figure 4, the number of displaced atoms in the fourth consecutive event is larger than in the single radiation event. The ratio of the total numbers of displaced atoms during the fourth consecutive event and the single event in figure 4 is approximately 1.7.

It appears that the damaged structure is less able to resist the damage, in that a consecutive radiation event that occurs in the structure that is already damaged results in a larger number of displaced atoms (calculated by comparing the final structure and the damaged structure before the consecutive event). The second observation from figure 4 is that the lifetime of the thermal spike phase is larger in the repeated event than in the single event, approximately by a factor of two. This means that the time of return to equilibrium positions by athermal relaxation reduces when the atoms are not located on the ideal lattice positions before the radiation event, having been displaced before. This suggests that the value of the ‘return’ potential is effectively reduced in the damaged structure and the response of the structure becomes more ‘loose’ in that sense.

We plot the dependence of the number of displaced atoms N_d on the total energy of implanted radiation damage events in figure 5. As can be seen from that figure, after five

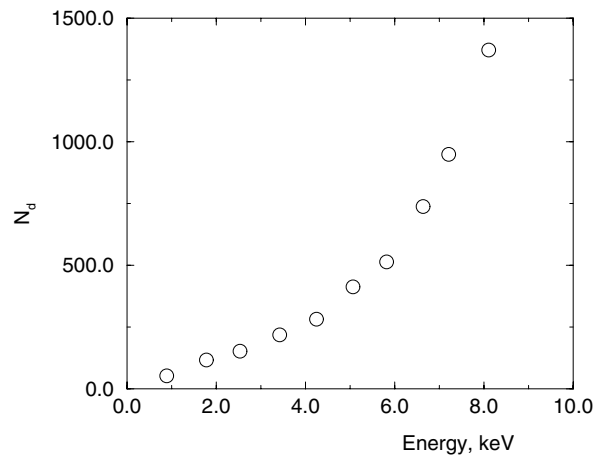


Figure 5. Number of displaced atoms as a function of total implanted energy, resulting from the simulation of several consecutive radiation events of approximately 1 keV each.

events have been implanted, corresponding to the total energy of about 4.5 keV, the number of displaced atoms becomes essentially non-linear. This is because the consecutive radiation events affect the regions already damaged by previous radiation events.

5. Density variation in the damaged region

For the damaged region, we calculate the number of atoms n that are located within the sphere with the centre defined as the geometrical centre of mass of the displaced atoms, together with n_0 for atoms located on undistorted lattice sites, and plot the relative difference $\Delta n/n_0 = (n - n_0)/n_0$ as a function of sphere radius in figure 6. Note that $\Delta n/n_0$ is plotted in figure 6 starting from about 4 Å. At the lower values of distance there are not enough atoms in the simulation sphere to produce statistically reliable values of $\Delta n/n_0$, which results in the strong noise in the interval 0–4 Å.

As can be seen from figure 6, the density of the damaged region becomes very close to that of the undistorted region beyond about 6 Å in the radial direction, up to the boundaries of the damaged region of 15 Å. A 10–15% increase in $\Delta n/n_0$ can be seen up to 6 Å in the radial direction, giving 12 Å as the characteristic size of the densified region. The densified region occupies a relatively small 6% portion of the total volume of the damaged region. Later we will relate the densification in the core of the damaged region to the appearance of connected SiO_n polyhedra.

It should be noted that the experimental measurements show that the macroscopic swelling in heavily damaged zircon reaches some 18% (see, for example, [3]). As mentioned earlier, we developed a model that, among other features, described the macroscopic swelling of irradiated material based on the assumption that locally the damaged region prefers to occupy a larger volume than that of the crystalline region [9]. The relaxation of the structure containing damaged and crystalline regions showed that at low dose the tensile stress from the damaged region is balanced by the compressive stress from the surrounding crystalline lattice which results in insignificant swelling. The balance changes as the relative amount of damage increases, resulting in gradual local swelling of the crystalline and damaged regions and the whole sample. However, the microscopic origin of the local swelling was not important in

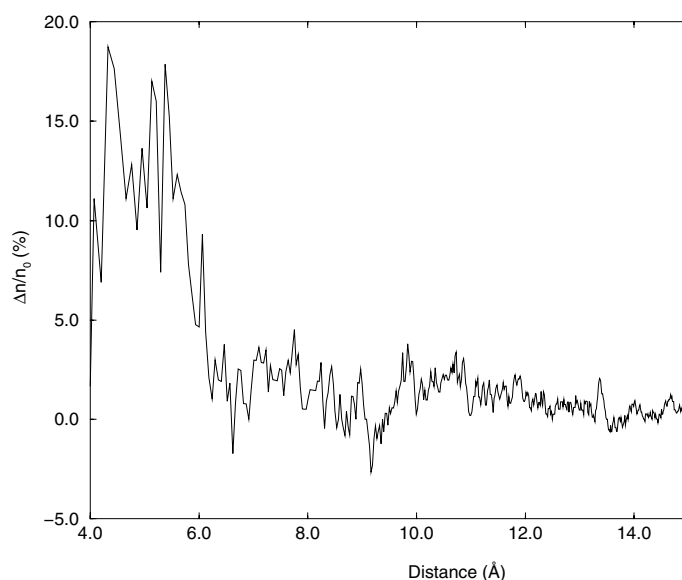


Figure 6. The change in relative number of atoms $\Delta n/n_0$ as a function of distance from the centre of the damaged region.

the formalism of [9]. The results of the atomistic simulation presented here suggest that the mere transition from the crystalline to the heavily damaged phase may not be accompanied by local swelling. Factors other than the introduction of topological disorder (embedding of point defects, irradiating particles and heavy ions into the structure etc) could be considered as regards their contribution to the microscopic origin of local swelling, thus making it a subject for future work.

6. 'Polymerization' in the damaged structure

The structure of the damaged region reveals an interesting feature: 'polymers' in the form of connected SiO_n ($n = 4, 5, 6$) polyhedra have appeared. During multiple-collision processes, SiO_4 tetrahedra which are separated in ideal zircon distort and move relative to each other, which enables them to share one or two common oxygen atoms, thus corresponding to vertex- or edge-sharing polyhedra. The radial distribution function was calculated for displaced Si atoms and for those in the undistorted zircon structure and is plotted in figure 7. As can be seen from figure 7, a new maximum in the radial distribution function at ~ 3 Å has appeared in the damaged structure. This new maximum is very close to the average Si–Si distance in silicates with linked SiO_4 tetrahedra, and corresponds to Si–Si neighbours in connected 'polymers'. The spread of Si–Si distances arises because of different orientations of polyhedra connected in chains in the damaged zircon structure.

An example of connected SiO_n polyhedra is plotted in figure 8. As can be seen from figure 8, the majority of connected polyhedra are fourfold and fivefold coordinated, with some six-coordinated polyhedra appearing. An oxygen atom which was forced away during multiple collisions forms a bond with another Si atom, and thus contributes to the observed increased coordination. Sharing of two oxygen atoms between two polyhedra also increases local coordination number (see figure 8). Note that the Si–Si distance between two polyhedra

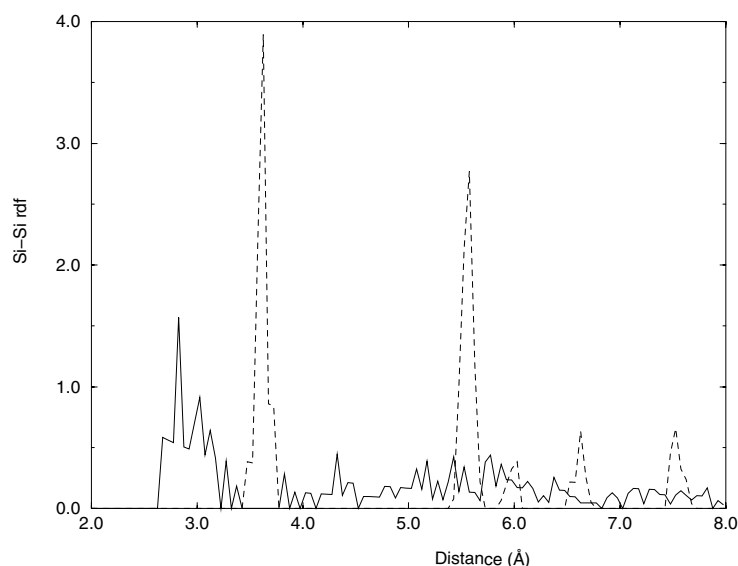


Figure 7. Si-Si radial distribution functions calculated for atoms in crystalline zircon and damaged structure.

that share two oxygen atoms (edge-sharing polyhedra) may be different from the Si-Si distance in vertex-sharing polyhedra. This contributes to the broadening of the first Si-Si peak in figure 7.

It is interesting that in our simulations the structure damaged by one radiation event contains mainly chains consisting of two or three connected polyhedra, while in some more heavily damaged structures up to 15 polyhedra connected in one chain are observed, vertex or edge sharing. This is consistent with the recent NMR studies of the structure of damaged zircon [13, 14] which pointed to the presence of connected SiO_4 tetrahedra. The average number of tetrahedra connected into chains was observed to increase in heavily damaged samples relative to slightly damaged ones [14]. It should be noted that the possibility for Si atoms to connect with each other by sharing O atoms was pointed out in [11].

A detailed study of the structure of disordered regions reveals that the alignment of the chains of connected SiO_n polyhedra is not completely random, as it might appear from figure 8. Figure 9 illustrates how SiO_4 tetrahedra that are separated in undamaged zircon may connect into ‘polymers’ when the damage is introduced. In the ideal zircon structure the nearest Si-Si distance is the shortest along the x - and y -directions and therefore these are more preferable directions for alignment of SiO_n chains than the z -direction, along which two nearest Si atoms are separated by a Zr atom. Once connected, polyhedra move and rotate according to local stresses in the damaged structure, but their alignment often has some ‘memory’ of the structure of the undamaged crystal. The animation showing how polyhedra connect into chains is available in MPEG format in the electronic version of this journal and can be downloaded from <http://www.esc.cam.ac.uk/movies>.

It is interesting to investigate the stability of SiO_n chains on longer annealing. The structure damaged at 300 K was annealed in stages up to 1800 K for about 300 ps, and the majority of polyhedra were found to remain stable and connected. However, a small fraction of the polyhedra that formed a chain became disconnected from their chain after a long annealing and, interestingly, chains that are disconnected from each other may form a larger connected

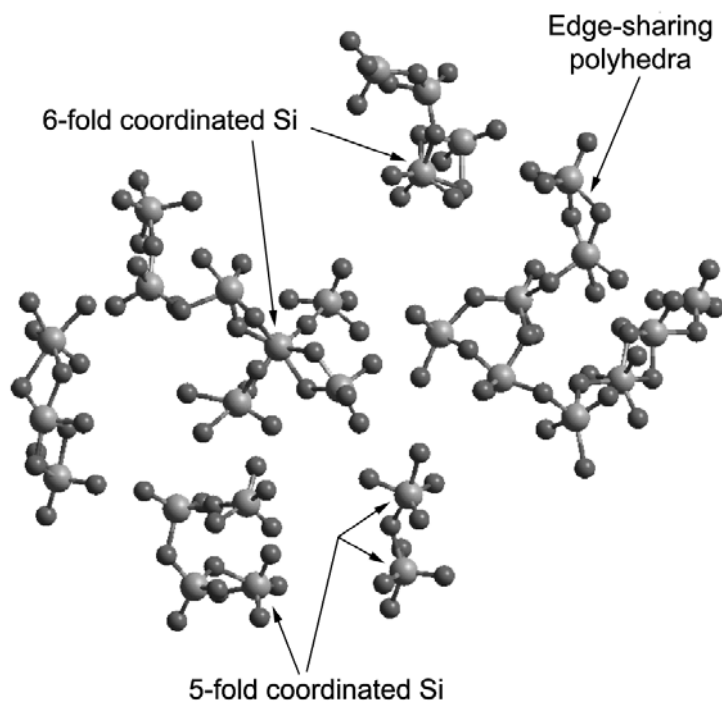



Figure 8. Connected polyhedra in the damaged region of zircon, showing 2, 3, 4, 7 and 9 polyhedra sharing one or two common oxygen atoms. Larger light balls represent Si atoms and smaller dark balls represent O atoms. Animation of the process of ‘polymer’ formation in zircon is available in the MPEG format in the electronic version of the journal (see below). It can also be viewed from <http://www.esc.cam.ac.uk/movies>.

 An MPEG movie of this figure is available from the article’s abstract page in the online journal; see www.iop.org.

‘polymer’. Thus the chains of polyhedra may evolve on annealing, but still retain the ‘polymer’ structure. It should be noted that the damaged regions observed experimentally relax over periods as long as many years while typical computer simulation times do not exceed several hundreds of ps. In this respect the ‘stability’ of the damaged structure may be considered on the timescale accessible in computer simulations only.

We relate the connection of SiO_n polyhedra into chains to the observed densification in the cores of damaged regions. Indeed, connecting the units that have been separated in the undistorted structure into chains leads to the local contraction of the volume and it is likely that the maximum contraction will be in the area with a high population of SiO_n chains. The size and location of the region that contains SiO_n chains was found to be approximately the same as the size and location of the densified core of the damaged region. This suggests that ‘polymerization’ may contribute to the microscopic mechanism behind the increase in density in the core of the damaged regions.

7. Summary

In summary, we simulated the response of the zircon structure to radiation damage and described the creation and development of displacement cascades. We demonstrated that

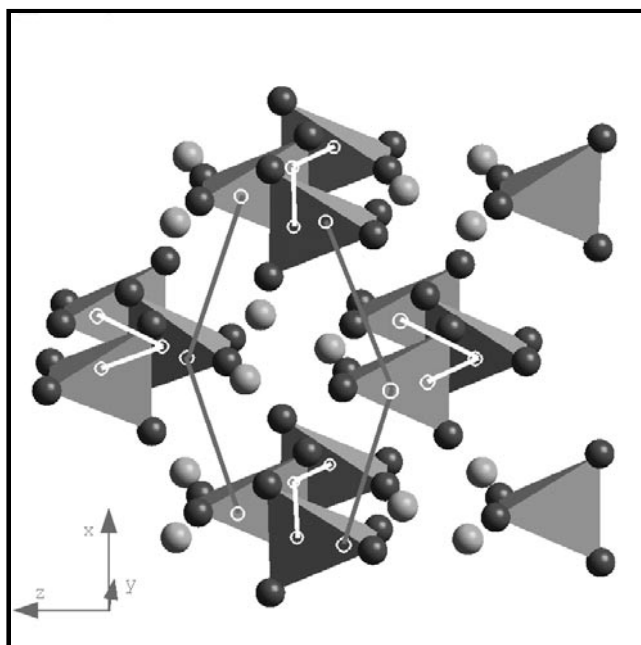


Figure 9. An illustration of directions along which SiO_4 tetrahedra, separated in undistorted crystalline zircon, connect into the chains of polyhedra. Grey balls represent Zr atoms.

the higher ambient temperature substantially reduces the number of displaced atoms during both the ballistic and the thermal spike phase. Several consecutive radiation events have been simulated in the adjacent regions of the structure and the overlap of the displacement cascades has been studied. It has been found that the damaged structure appears to be less resistant to further radiation damage, in that more damage is created by an event with the same energy and the relaxation time increases.

The study of the damaged structure has revealed the formation of 'polymers' in the form of SiO_n , $n = 4, 5, 6$, polyhedra that are connected via one or two shared oxygen atoms. It has been found that the orientations of 'polymers' may preserve the directions of alignment of SiO_4 tetrahedra in undistorted zircon. The simulation of annealing of the damaged structure has shown that the 'polymers' are essentially stable formations. The calculated densification in the core of the damaged region has been suggested to be promoted by the connection of SiO_n polyhedra into chains.

Acknowledgments

We are grateful to the EPSRC for financial support, and KT is grateful to the Cambridge Overseas Trust for support. The calculations were performed using the Hitachi computers of the High Performance Computing Facility in Cambridge.

References

- [1] Chakoumakos B C, Murakami T, Lumpkin G R and Ewing R C 1987 *Science* **236** 1493
- [2] Murakami T, Chakoumakos B C, Ewing R C, Lumpkin G R and Weber W J 1991 *Am. Mineral.* **76** 1510

- [3] Weber W J, Ewing R C and Wang L M 1994 *J. Mater. Res.* **9** 688
- [4] Meldrum A, Boatner L A and Ewing R C 1997 *Phys. Rev. B* **56** 13 805
- [5] Meldrum A, Zinkle S J, Boatner L A and Ewing R C 1999 *Phys. Rev. B* **59** 3981
- [6] Zhang M, Salje E K H, Capitani G C, Leroux H, Clark A M, Schluter J and Ewing R C 2000 *J. Phys.: Condens. Matter* **12** 3131
- [7] Rios S, Salje E K H, Zhang M and Ewing R C 2000 *J. Phys.: Condens. Matter* **12** 2401
- [8] Rios S and Salje E K H 1999 *J. Phys.: Condens. Matter* **11** 8947
- [9] Trachenko K, Dove M T and Salje E K H 2000 *J. Appl. Phys.* **87** 7702
- [10] Crocombette J P and Ghaleb D 1998 *Mater. Res. Soc. Symp. Proc.* **506** 101
- [11] Crocombette J P and Ghaleb D 1999 *Mater. Res. Soc. Symp. Proc.* **540** 343
- [12] Park B, Corales L R and Weber W J 1999 *Mater. Res. Soc. Symp. Proc.*
- [13] Farnan I 1999 *Phase Transitions* **69** 47
- [14] Farnan I and Salje E K H 2001 *J. Appl. Phys.* submitted
- [15] Sanders M J, Leslie M and Catlow C R A 1984 *J. Chem. Soc., Chem. Commun.* 1271
- [16] Pryde A K A, Hammonds K D, Dove M T, Heine V, Gale J D and Warren M C 1996 *J. Phys.: Condens. Matter* **8** 10 973
- [17] Gale J D 1997 *J. Chem. Soc., Faraday Trans.* **93** 629
- [18] Mittal R, Harris M J and Bull M J 1997 *Rutherford Appleton Laboratory ISIS Experimental Report No* 8919
- [19] Smith W and Forester T 1996 *J. Mol. Graph.* **14** 136
- [20] Bacon D J, Calder A F and Gao F 1997 *J. Nucl. Mater.* **251** 1
- [21] Bacon D J, Gao F and Osetsky Y N 1999 *Nucl. Instrum. Methods Phys. Res. B* **153** 87
- [22] Nordlund K, Ghaly M, Averback R S, Caturla M, Diaz de la Rubia T and Tarus J 1997 *Phys. Rev. B* **57** 57
- [23] Bacon D J, Gao F and Osetsky Y N 2000 *J. Nucl. Mater.* **276** 1